ELSEVIER

Journal of Nuclear Materials 266–269 (1999) 1273–1278

journal of nuclear materials

Plasma–wall interaction in the Spanish stellarator TJ-II. Diagnostics and first results

F.L. Tabarés [a,*], D. Tafalla, E. de la Cal, B. Brañas, TJ-II team

[a] *Asociación Euratom/Ciemat, Av Complutense 22, 28040 Madrid, Spain*

Abstract

First plasmas have been produced in the Spanish stellarator TJ-II. They have been generated by 250 kW ECR heating under all metal wall conditions. Two different magnetic configurations, corresponding to similar iota values but different plasma volumes, have been used. Helium glow discharge conditioning has been systematically applied previous to and between discharges. Good plasma start-up performance has been obtained, characterised by a short delay respect to the gyrotron pulse and controlled peak value of the electron density. The present results stress the important role that plasma–wall interaction phenomena are expected to play in the generation and optimisation of TJ-II plasmas in future campaigns.

Keywords: TJ-II; Stellarator; ECH

1. Introduction

TJ-II is a medium size helical axis stellarator located in CIEMAT, Madrid [1], whose main parameters are: $R = 1.5$ m, toroidal field at the axis of 1 T and the pulse length varies from 0.2 to 0.5 s, with a discharge repetition rate of one every 5 min. One of its main characteristics is a high flexibility in magnetic configurations ($0.96 <$ iota < 2.5, $1\% <$ shear $< 10\%$, $-1\% <$ magnetic well $< 6\%$). That is achieved by the separate control of a set of five different types of coils, which include the 32 toroidal field coils centred around a four-period toroidal helix, a circular coil located at the major axis and a helical winding wrapped around the circular one, following the same winding law as the toroidal coils. Plasma heating is achieved by means of up to 700 kW ECRH at 53.2 GHz (two lines) in the initial experimental phase and up to 4 MW NBI in the high beta ($<5\%$) phase. Bean-shaped plasmas with average minor radius $a < 0.22$ m (plasma volume <1.4 m^3) are produced in this way.

2. Vacuum vessel, pumping and glow discharge systems

The vacuum vessel (VV) of the TJ-II has been described in previous works [2]. Briefly, it is made of certificated nonmagnetic austenitic stainless steel and composed of 32 sectors and 32 rings distributed into four equal periods. Connection between these components is made by a continuous weld at the inner side. An octant of the VV, showing some of the characteristic components, is displayed in Fig. 1. The vessel volume without diagnostics is 6 m^3, and the total inner area including thermal protections (see below) is $\approx$75 m^2. Access for diagnostics, poloidal limiters, pumping and plasma heating systems is provided by 96 trapezoidal ports of different sizes. Each of these ports has two types of sealing, a $\phi = 4$ mm Helicoflex HN 200 gasket (inner side) and a $\phi = 4$ mm Viton O-ring (outer), so allowing quick leak checking of the whole flange. The total leak rate of the vacuum chamber after the final welding of the octants at he CIEMAT was below 10^{-9} mbar l/s. The cleaning cycle of the inner walls of the vessel includes chemical cleaning with RBS 350 and baking of the whole VV at 150°C. This baking will be carried out by eddy current induction by applying AC current (50 Hz, 559 V, 242 A) to the toroidal field coils. Electrical heaters are installed in ports and torus appendages to compensate

* Corresponding author. E-mail: paco.tabares@ciemat.es

0022-3115/99/$ – see front matter
PII: S0022-3115(98)00861-7

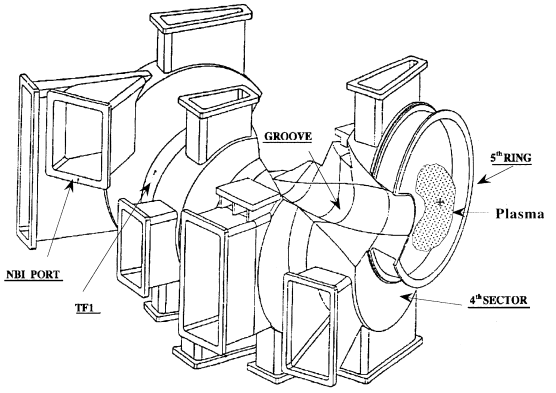

Fig. 1. An octant of the TJ-II vacuum vessel. The structure is based on a combination of rings and sectors, the latter carrying the observation and heating ports. The indentation (groove) allows for a close coupling of the VV to the central coil system. The plasma, with its characteristic bean shape, is also schematically shown.

for heating nonuniformity. Control of the full system is based on an artificial neural network. Although the system was not used in the initial phase here described, testing in a sector of the vessel indicates deviation of local temperature values in the range of ±15°C.

The vacuum system [3] consists of a set of four symmetrically spaced turbomolecular pumps with nominal pumping speed of 1600 l/s (N_2) each. They are coupled to the VV through bottom ports having the maximum conductance (4760 l/s). This setup yields an effective pumping speed of ≈4000 l/s at the vessel. Typical base pressures below 10^{-7} mbar are achieved for the present (unbaked, full metallic) conditions. The analysis of residual gases under high vacuum conditions is made with a residual gas analyser (RGA) installed directly in the TJ-II vacuum vessel with a heated, high conductance connection. The gas injection system (GIS) consists of eight fast piezoelectric valves, symmetrically located around the vessel. It is able to deliver gas fluxes above 100 mbar l/s, with a time response of a few milliseconds. In its initial configuration only preprogrammed operation was available. Fluxes were inferred from the pressure rise into the chamber, as measured by a fast ionisation gauge.

The conditioning of the vacuum vessel previous to the initial experimental campaign was performed by helium glow discharge cleaning at room temperature, as baking of the vessel was not yet available. The glow discharge is carried out by applying a DC voltage of about 300 V to two L-shaped stainless steel anodes, spontaneously refrigerated and fixed into the vessel. The total discharge current is typically 1 A per anode, equivalent to a current density of about 4 μA cm^{-2}. The discharge is started up by applying a DC voltage of 1000 V and with the help of a short injection of argon. When the glow is started, the argon injection is switched off and the discharge is sustained at helium pressures of 5×10^{-3} mbar using a feedback-controlled gas injection system. At this pressure the pumping speed of the vacuum system is about 2400 l/s. A quadrupole mass spectrometer, differentially pumped and connected to the TJ-II vacuum vessel through a low conductance hole and pipe setup, allows us to analyse the evolution of gas species produced during the conditioning discharge. Both, the mass spectrometer and the sampling systems, are heated to 150°C during the measurements. The system is absolutely calibrated for different gases.

3. Plasma–wall interaction

One of the main characteristics of the TJ-II plasmas is their strong interaction with the region of the chamber (groove) surrounding the hard core coil, as schematically shown in Fig. 1. In fact, this part of the vessel represents the main limiter under the most magnetic configurations, although the poloidal location of the specific interaction region evolves with iota values [1]. For low (≈1) values, an almost pure tangential interaction, centred respect to the helical middle plane, is expected. At higher iota values, corresponding to higher plasma volumes, a splitting of the interaction area takes place, its location corresponding to higher poloidal angles for higher iota values. Although some degree of toroidal asymmetry is predicted by the calculations, no hot spots in the groove area are foreseen in principle for most configurations. Only in some extreme configurations (fat plasmas), the steps formed in the transition from chamber module to closing ring can be the limiting element, instead of the groove area. In order to protect the groove region during plasma shots, a thermal shield has been installed. The design of that shield was optimised with respect to virtual leaks and transient outgassing but allowing a good thermal contact.

For the NBI heating scenarios, local thermal loads directly arising from the intersection of the beams with the vessel components are expected to dominate over those due to the plasma interaction, including fast orbit losses [4]. The overall situation is summarised in Table 1. As seen, maximum loads in the presence of plasmas are expected in the injection port (TF-1) and in the region of the vessel marginally touched by the beam in its path. Peak values up to ≈1 kW/cm^2 are expected during plasma operation. Due to the relatively short duration of the beam injection, these high loads correspond to moderate peak temperatures (<1000 K) if typical carbon materials are used to protect the corresponding regions. Also seen is the compensating effect that shine through and plasma induced loads have on

Table 1
Summary of the estimated thermal loads in critical parts of the vacuum vessel during the NBI heating of TJ-II plasmas

	Peak power loads at TJ-II protections (W/cm^2, 930 kW per beam inside the torus, 40 keV)					
	TF-1	PLT-56	PLT-45	PLT-55	HC only shine through	HC all loads[a]
No plasma	850	1900	1100	920	570	570
(total power, kW)	(90)	(400)	(90)	(240)	(200)	
Beam start (1.7×10^{19} m^{-3})	850	770	730	400	410	420[b]
Intermediate density (5×10^{19} m^{-3})	850	270	460	90	200	220
High density (10^{20} m^{-3})	850	80	410	12	70	390
Average in typical high density discharge	850 (90 kW)	350 (70 kW)	500 (55 kW)	150 (40 kW)	250 (90 kW)	360

The beam injection port is near the toroidal field coil TF-1, and the beam passes near some of the vertical flat plates existing between sectors and rings, as 45 and 56, as sketched in Fig. 1. See Ref. [4] for more details.
[a]All loads: Shine through, plasma, CX neutrals, fast ions.
[b]ECRH plasma loads in HC (≈100 W/cm^2) not included as they do not overlap in space.

total loads to the groove thermal protection as plasma density is increased.

In order to reduce the interaction between the plasma and the vessel when required, four mobile limiters have been constructed [5], although only two of them have been installed in the initial phase. They are located in lower machine ports, at 180° toroidally. They can be moved 50 cm inside the chamber and be inclined ±15° from the horizontal plane to accommodate all possible plasma shapes. The limiter heads, which for the initial phase consist of 10 stainless steel tiles (2 cm poloidally and 9 cm toroidally each), are exponentially shaped in the toroidal direction in order to get a constant power density distribution. Langmuir probes and thermoresistances are embedded in the tiles (see Section 4).

4. Edge diagnostics

The characterisation of the edge and SOL regions of the TJ-II plasmas under all possible configurations is one of the critical points to be pursued experimentally. A set of diagnostics with the required flexibility has been developed for that purpose. Due to expected presence of poloidal and toroidal asymmetries, several equivalent locations of the plasma periphery need to be characterised. In addition, the large distance existing between the flanges, where the diagnostic is mounted, and the plasma (typically > 70 cm) has required in many instances the development of novel designs. Several types of Langmuir probes are employed. A set of four pin probes, that can be operated under different combinations, are installed in the movable limiters, providing single shot recording of n_e and T_e profiles (six points radially, three poloidally) at the plasma periphery. A fast reciprocating Langmuir probe has been developed and constructed. The fast stroke, pneumatically driven, has a length of 0.1 m at a speed of 1.5 m/s. The system's head can be extracted by a vacuum valve and exchanged for the different experiments (replace damaged pins, heads with Langmuir and magnetic probes, etc.). In addition, fixed probes, attached to critical regions of the VV, are presently being designed.

Optical diagnostics are widely used in TJ-II for the characterisation of plasma–wall interaction and edge parameters. A set of H_α detectors, relatively calibrated, are used to monitor the gas injection at four toroidal positions and the recycling at selected locations, including the four limiters and some regions of the groove. Two photodiode arrays (38 pixels) are used for the monitoring of the spatial distribution of the recycling neutrals near the limiters. A CCD camera in combination with selected interference filters [5] provides 2D information of edge parameters and recycling at the mobile limiters. IR thermography of such limiters is presently being developed.

A strong effort has been devoted to the development of active optical diagnostics in TJ-II. Two laser induced fluorescence (LIF) diagnostics have been implemented. The first, based on a flashlamp pumped dye laser, provides H_α laser radiation (1 J/pulse, 1 μs) to be used for neutral H profile determination under different operational scenarios. That information, together with passive spectroscopy and Montecarlo simulation, will be used for the understanding of particle transport. The second LIF diagnostic is based on an excimer pumped dye laser. In the first harmonic it provides tunable radiation in the range 350–750 nm, suitable for the pumping of metallic impurities, with a typical spatial resolution of few millimetres. A SHG setup allows for the generation of UV radiation, of potential use in metallic ion detection. Two types of atomic beams are presently installed in TJ-II. A thermal Li beam, produced from an effusive oven, will provide information on the SOL profiles at two poloidal positions. Recording of the Li emission will be made through a multianode PM (16 channels), thus allowing

for continuous recording of the electron density profile. A newly developed supersonic He beam [6] will be used for the determination of electron density and temperature profiles in the edge and SOL regions. Its typical divergence is 1°, thus allowing for good spatial resolution even when its coupling to the TJ-II implies a fairly high distance between the source and the plasma (≈70 cm). A He pulse length of < 3 ms and a repetition rate of ≈50 Hz will be typically used. Simultaneous detection of the three He lines used for the reconstruction of the edge profiles (667.2, 706.5 and 728.1 nm) is made through a set of photomultipliers and a rotating mirror. In addition to them, several types of spectroscopic diagnostics and a differentially pumped mass spectrometer with typical response time of ≈40 ms are used.

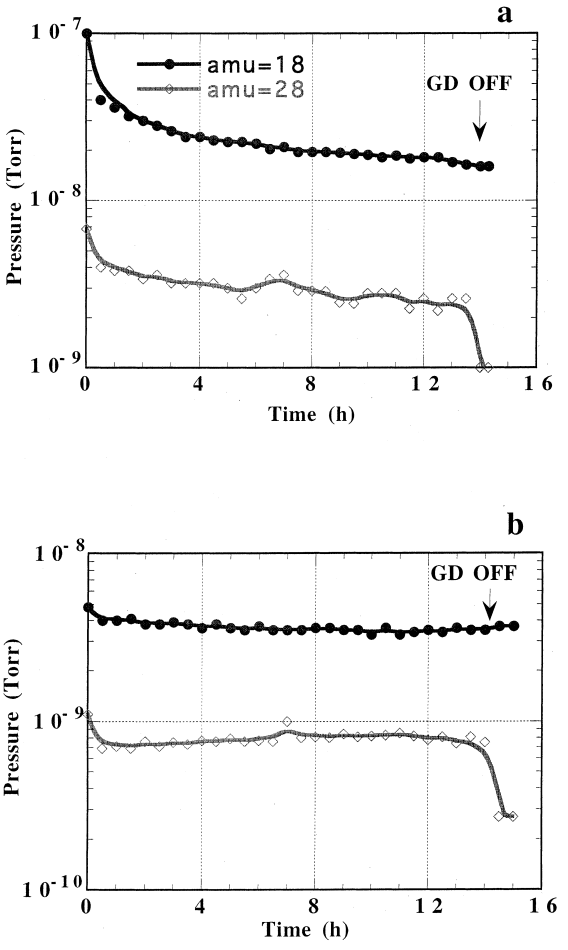

Fig. 2. Evolution of water and CO characteristic peaks during He GDC of the vacuum chamber. (a) Before plasma operation. (b) Between operations. The signals are directly taken from the differentially pumped mass spectrometer. No transmission factors are included.

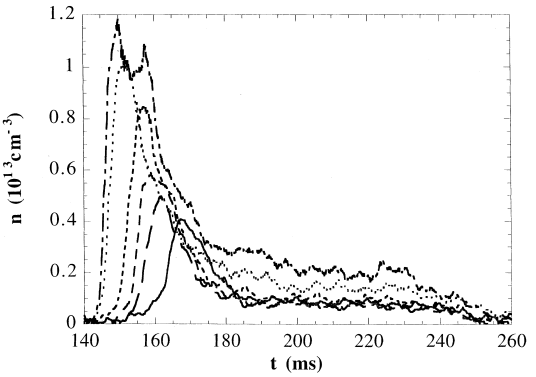

Fig. 3. Time behaviour of the line average electron density for a fixed hydrogen base pressure of 2×10^{-5} mbar (N_2 eq.) after the injection of a 250 kW, 90 ms ECRH pulse, at 140 ms. From left to right, the central toroidal field value is decreased in a 1% respect to that corresponding to the resonance for the EC frequency (0.95 T for 53.2 GHz).

5. Initial operation

In the start-up campaign, only ECRH (53.2 GHz, 250 kW, 80–100 ms) has been used for the initiation and heating of the plasma. Two magnetic configurations were generated, the corresponding minor radii being 11.6 and 14.9 cm, respectively. The iota value for both cases is 1.5–1.6. An overview of the plasma performance during this phase will be presented elsewhere [7], and only details about density control and impurity generation are presented here. Glow discharge conditioning was applied to the chamber before the initiation of the campaign and overnight, between operating days. Fig. 2 shows the time evolution of typical impurity peaks along the cleaning period. As it can be seen, a much stronger impurity release is observed during the cleaning of the chamber before plasma operation, for the same GDC parameters. The weak, and constant in time, release of typical impurities between discharges is consistent with the small contribution of desorbed species inferred by the particle balance in the density build-up phase of the plasma (see below). Mass spectra taken directly in the vacuum chamber after the GD show typical activated wall pumping behaviour, leading to a base pressure decrease of 10–20%. The recovery times for water and oxygen were found of the order of 1 and 20 h, respectively.

Hydrogen was injected through the GIS at different times during the ramp-up of the fields. Short pulses were used to provide the background pressure ($<2 \times 10^{-5}$ mbar, N_2 eq.) required for the ECRH start-up. The time delay respect to the MW pulse as well as the peak density were found very sensitive to the location of the resonance surface for EC absorption within the plasma centre, i.e., the central TF value. In Fig. 3, the time

behaviour of the line average electron density is shown for different values of the toroidal field, at constant hydrogen pressure at the time of MW injection. A weaker dependence was found for plasmas configurations with larger minor radius. As seen, delays between 2 and 20 ms are achieved, depending on conditions. Taking into account the nominal plasma volume and assuming a parabolic density profile, the peak density observed corresponds to ionisation of 40% of the gas. For optimum field values, the peak density value was a weak function of the initial pressure, but a cold plasma typically lasting ≈20 ms was formed at the beginning for filling pressures above a critical value. For the cases of fast density rise, no densities above the limit due to the hydrogen particle balance were obtained, thus suggesting a small contribution of impurity sources in the initial phase of the discharge.

The evolution of some significant plasma parameters during the ECR heating pulse (250 kW in both cases) is shown in Figs. 4 and 5 for two magnetic configurations. Absolute values are given only for the line average electron density. Only characteristic lines from low Z impurities are reported here, although traces of neutral metallic impurities were also detected for other detection geometries. Even when the density built-up phase is similar in both cases (density rise, time delay respect to gyrotron pulse and H_α evolution), a remarkable different time evolution of the respective plasmas can be observed afterwards. In spite of the fact that hydrogen is introduced as a short pulse, well before the injection of MW, a density plateau is obtained in both cases. Due to the expected limited recycling conditions of the He conditioned metallic walls, this suggests a significant contribution of impurities to the plasma fuelling at longer

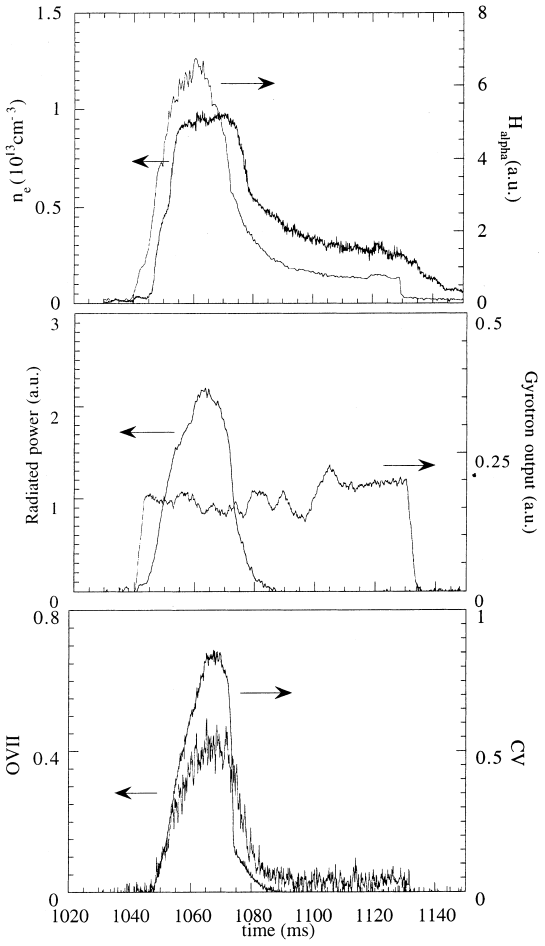

Fig. 4. Typical traces of some representative diagnostics during the start-up phase of TJ-II: electron density, H_{alpha}, bolometer signal, EC radiometer and two impurity detectors (CV dashed line, right scale, OVII continuous, left scale). Magnetic configuration with $\langle a \rangle = 11.6$ cm.

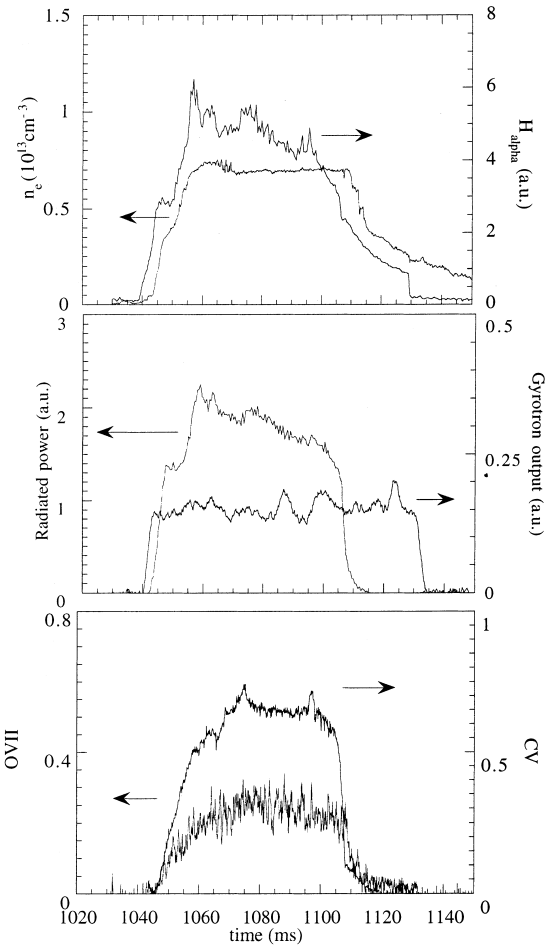

Fig. 5. Same as Fig. 4 for a magnetic configuration with $\langle a \rangle = 14.9$ cm.

times. The total radiation monitor closely follows the time behaviour of the displayed plasma impurities, and its drastic decay before the termination of the heating pulse, for values of electron density well below the cut-off limit, point to the presence of raditative collapses in these start-up plasmas. The longer time required for such a collapse to take place in the plasmas generated in the magnetic configuration corresponding to a larger volume, but with similar nominal limiting area, stresses the importance of plasma–wall interaction control for the exploitation of the full capabilities of TJ-II in the future. For that purpose, low Z operational scenarios are being presently prepared.

6. Conclusions

First plasmas have been produced in TJ-II under pure ECRH conditions. Only metallic components were exposed to the plasma, and the chamber was conditioned by He GDC. Good control of the preionisation of the injected gas (hydrogen) by the MW pulse was achieved, with typical delays of the density built-up of a few milliseconds. The duration of the plasma pulses was limited by radiative collapse due to impurity generation. Plasmas with larger volumes, to be generated in future campaigns, are critically less affected by the plasma–wall interaction effects.

References

[1] C. Alejaldre et al., Fusion Technol. 17 (1990) 131.
[2] J. Botija et al., Proceedings of the 17th Symposium on Fusion Technology, Rome, 1992, p. 201.
[3] F.L. Tabarés, A. García, J. Botija, Vacuum 45 (1994) 1059.
[4] J. Guasp, C. Fuentes, M. Liniers, Report CIEMAT-797, May 1996.
[5] E. de la Cal et al., these Proceedings.
[6] F.L. Tabarés, D. Tafalla, V. Herrero, I. Tanarro, J. Nucl. Mater. 241–243 (1997) 1228.
[7] C. Alejaldre and the TJ-II Team, First plasmas in the TJ-II flexible heliac, to be presented in the 25th EPS Conference, Prague, 1998.